

Aluminum (III) Interactions with Sulfur-Containing Amino Acid Chains

Jose M. Mercero,[†] Arantxa Irigoras,[‡] Xabier Lopez,[†] Joseph E. Fowler,[†] and Jesus M. Ugalde^{*,†}

Kimika Fakultatea Euskal Herriko Unibertsitatea, P. K. 1072, 20080 Donostia, Euskal Herria, Spain, and Humanitateak eta Hezkuntza Zientzien Fakultatea, Mondragon Unibertsitatea, Dorleta auzou, z/g, 20540 Eskoriatza, Euskadi, Spain

Received: March 29, 2001

In this paper, we have extended our studies concerning aluminum (III) and amino acid chain interactions. We focus on the sulfur containing amino acid chains of cysteine (Cys) and methionine (Met) and analyze the interactions with the toxic aluminum (III) and the nontoxic magnesium (II) cations. We start with the simplest model representing the amino acid and complete it adding methyl groups to model more accurately the amino acid chain. We compare the results obtained for both cation complexes. Mg(II) was found to bind to all of the neutral ligands in this study with binding energies of 79, 97, 109, and 120 kcal/mol for SH₂, HSCH₃, CH₃SCH₃, and CH₃SCH₂CH₃, respectively, while Al(III) bound only to the largest of these ligands (binding energy: 383 kcal/mol) and then in a bidentate form with a bond to both S and the terminal C. The binding to the anionic ligands was much stronger; binding energies of 351 and 360 kcal/mol are predicted for Mg(II) binding to SH⁻ and SCH₃⁻, respectively; for Al(III) those values are 702 and 741 kcal/mol. We also study the differences between these complexes and the complexes formed between these metal cations and the acid and acid derivative amino acid chains studied in earlier works.

Introduction

Because of the reports of aluminum (III) cation negative aspects in biological systems, a significant number of studies concerning this cation have been performed,¹ many of which focused on the path taken by aluminum to enter the cell.^{2–5} Aluminum is thought to interfere in biological systems through competition with other metal cations. It is seen to enter and permanently occupy binding sites which in healthy systems are served by other metal cations with specific binding and charge properties.⁶ Magnesium (II) seems to be the most affected cation, since the two cations are similar in size, which is a dominant factor over the charge identity in terms of metal ion competition.^{7,8}

Metal cations and amino acids *ab initio* studies are not abundant in the literature, especially lacking are reports including aluminum interactions. There are some studies concerning dications and amino acids interactions.^{9–12} Garmer and Gresh studied the differences between hard and soft cations binding to biological ligands.^{9,11} Deerfield et al.¹² studied the first solvation shell of magnesium (II) in a protein environment giving a reasonable model for the interior of a protein. Yañez's group has also studied the reactions between some monocations and formamide^{13,14} using *ab initio* methodology and comparing their theoretical results with mass spectrometry investigations for the Cu(I) case.¹⁵

Previously, we have investigated the interactions between aluminum (III) and both acidic¹⁶ (aspartic acid and glutamic acid (Asp and Glu)) and acid derivative amino acid chains¹⁷ (asparagine and glutamine (Asn and Gln)) comparing our results to equal levels of theory applied to magnesium (II) interactions with the same species. We observed that the binding energies

for aluminum (III) are significantly larger than magnesium (II) ones, and that the strongest bindings occurred with the Asp and Glu amino acid chains. An important difference between both cations was given for the acidic amino acid–metal complexes. According to the NBO analysis, while the aluminum forms Lewis-type bonds to the ligand, the magnesium is bound only by second-order interactions.¹⁶ Similarly, the Bader analysis reported covalent bonds for the aluminum complexes while magnesium bonds were described as being ionic.¹⁷

In the present study we will focus on the sulfur containing amino acids, cysteine (Cys) and methionine (Met). We have used the sulfidric acid and methylthiol to represent the Cys side chain, and SH⁻ and methanethiolate to represent the deprotonated Cys, which is a common residue in metal binding sites. Deprotonated Cys has also been observed at the active site of the cysteine protease enzyme¹⁸ and in the mercaptan-like metalloenzyme inhibitors.^{19,20} Methionine has only been found binding to copper ions in proteins. CH₃–SHCH₃ and CH₃–SHCH₂CH₃ structures have been employed to simulate the Met side chain.

Methods

All calculations were carried out with the GAUSSIAN94²¹ and GAUSSIAN98²² packages. It has already been proven that the density functional methods give excellent results in most chemical systems.²³ The HF and DFT hybrid methods corrected the pure DFT overestimation of the bond dissociation energies²⁴ as was validated by Johnson et al.²⁵ The Becke proposed hybrid²⁶(B3), together with the LYP²⁷ correlation functionals have been chosen for this work.

The all electron 6-31G split valence basis set augmented with a diffuse sp set of functions and a polarization set of p and d functions has been used in this work (6-31++G**). Frequencies were calculated at this level of theory and the corresponding

[†] Kimika Fakultatea Euskal Herriko Unibertsitatea.

[‡] Mondragon Unibertsitatea.

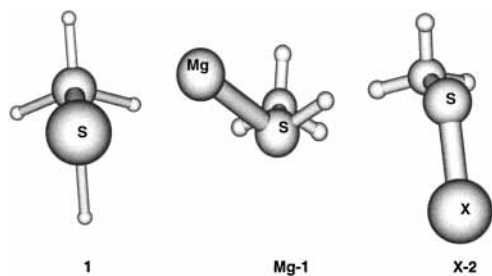


Figure 1. **1** is the minimum of the CH_3SH potential energy surface corresponding to the Cys amino acid chain; **Mg-1** is the minimum on the $\text{Mg-SHCH}_3]^+$ potential energy surface. **X-2** is the ground-state complex formed by the metal binding with the dehydrogenated Cys chain.

zero-point vibrational energy (ZPVE) corrections made to the total energy. The binding energy was evaluated with the ZPVE corrected energies as follows:

$$(B_e) = E_{xl} - (E_l + E_x) \quad (1)$$

where xl stands for the complex, x for the metal, and l for the ligand.

The natural bond orbital²⁸ analysis and the Bader²⁹ analysis were used to understand better the character of the corresponding cation–ligand interactions. Natural bond orbital analysis was performed on the polyatomic wave function³⁰ using the NBO program³¹ of the GAUSSIAN package and the natural charges of the atoms were also evaluated. This method localizes the molecular orbitals and provides data that are in good agreement with the concepts of Lewis structures and the basic Pauling–Slater–Coulson picture of bond hybridization and polarization. For a good review of NBO and its applications, see the review article by Reed, Curtis, and Weinhold.²⁸ The AIM-PAC³² package was employed to perform the Bader analysis.

The MOLDEN³² program was used to visualize and draw the figures.

Results and Discussion

We have first studied the interactions of Al(III) and Mg(II) with both the neutral and the anionic forms of cysteine, (since its pK is 8.5, it may lose the proton in the physiological environment) and the methionine chain. As in our previous studies,^{17,23} we start with the interactions between the smallest representation of the amino acid chain and the cation, and then we add a methyl group to represent the amino acid chains more precisely, i.e., first we studied the interactions between the metal and SH_2 (or the anionic form SH^-), then we included a methyl group to represent the complete Cys amino acid chain. Similarly, we study the $\text{CH}_3\text{SCH}_3\text{-X}$ interactions, and then add a methyl group to represent more accurately the Met amino acid chain. We have found many different stationary points on the corresponding potential energy surfaces but we focus our discussion on the corresponding minima. Geometries, natural charges, the Bader bonding properties, and the complexation energetics are shown in Tables 1, 2, 3, and 4 respectively.

X-Cysteine Amino Acid Chain Interactions. Neutral Form. The smallest functional group of Cys is sulfidric acid (SH_2). At the B3LYP/6-31++G** level of theory, the S–H bond length is 1.348 Å and the H–S–H angle is 92.75°.

After the addition of a methyl group, we have located two rotomers on the HSC_3 potential energy surface. The anti rotomer (see **1** in Figure 1) corresponds to the ground state, and the Gauche rotomer is a transition state, only 1 kcal/mol

higher in energy. The S–H bond length does not change while the H–S–C angle has a value of 97.05°. The charge distribution of the SH_2 rearranges after the addition of the methyl group. The sulfur lessens in negative charge from $-0.283e^-$ to $-0.052e^-$. The carbon has a negative charge of $-0.789e^-$ while the hydrogens of the methyl have a charge around $+0.24e^-$ (see Table 2).

Studying the interactions between this amino acid chain and both metal cations, we have not located any stable complex formed between SH_2 nor CH_3SH and the aluminum (III) cation. There does exist an $\text{AlSH}_2]^{\beta+}$ C_{2v} symmetry complex with an imaginary frequency, in which the B3LYP/6-31++G** wave function experiences RHF–UHF instability. Reducing the symmetry and reoptimizing led to dissociation, and the same was observed for CCSD/6-31++G** calculations. However, we did find a stable minimum structure for $\text{AlSH}_2]^{\beta+}$ at many other levels of theory, e.g., MP2/6-31++G**, B3PW91/6-31++G**, CCSD/6-311++G(2df,2p), etc. In all this minima the Al–S bond length is around 2.5 Å indicating a different type of a complex as compared with the Mg complex since the Al–S bond length is larger than the corresponding Mg–S bond. The potential energy function along the Al–S coordinate reveals a tiny potential energy well with a very small barrier of 0.6 kcal/mol toward dissociation into either $\text{Al}^+ + \text{SH}_2^{+2}$ or $\text{Al}^+ + \text{SH}_2^{+2}$ which are 107 and 173.14 kcal/mol lower in energy than the $\text{AlSH}_2]^{\beta+}$ complex, respectively. Moreover, this small barrier is unable to prevent spontaneous dissociation of the $\text{AlSH}_2]^{\beta+}$ into Al and SH_2^{+2} for the ZPVE of the calculated $\text{Al-SH}_2]^{\beta+}$ is 10 kcal/mol. Hence our calculations predict that the $\text{Al-SH}_2]^{\beta+}$ does not survive to the ZPVE correction and that the interaction of Al^{+3} with SH_2 leads to a charge-transfer reaction. A similar study was performed for the $\text{Al-SHCH}_3]^{\beta+}$ and $\text{Al-S(CH}_3)_2]^{\beta+}$ structures, resulting in no stable structure found at any of these levels of theory, namely, MP2(full) with 6-31++G** and aug-cc-pVTZ basis sets, B3PW91 with 6-31++G** and 6-31++G(2df,2p) basis sets and finally for CCSD with 6-31++G**, cc-pVTZ, and 6-311++G(2df,2p) basis sets.

In contrast, the magnesium (II) binds to both the sulfidric acid and its methyl-derivative. Two $\text{Mg-SH}_2]^{\beta+}$ structures have been located, a planar C_{2v} structure with an imaginary frequency which breaks the planarity, and a nonplanar C_s minimum which is 12 kcal/mol lower in energy. The Mg atom is 101.1° degrees out of the HSH plane. In this species the magnesium binds to SH_2 with a Mg–S bond length of 2.477 Å. The S–H bond length elongates slightly from 1.348 Å to 1.362, while the H–S–H angle opens from 92.76° to 100.01°. There is a charge transfer from the SH_2 hydrogens to the magnesium atom, which has a positive natural charge after complexation of $+1.731e^-$, and the hydrogens increase in positive charge by around 0.1 e^- . The Bader analysis of this minimum was performed, and according to this, the magnesium cation activates the S–H bonds, thus their energy density becomes less negative (see Table 3), and they elongate from 1.348 to 1.362 Å. The forming Mg–S bond is qualified as covalent since the energy density has a value of -0.002 au. The Natural bond analysis reports a bond between the sulfur and the magnesium. The former contributes with a 3p orbital lone-pair (87%) which forms the bond with the 3s empty orbital of the magnesium (II) cation which contributes with 13%. This 3p lone pair corresponds to the HOMO orbital of SH_2 which is located out of the SH_2 plane. Thus, the $\text{MgSH}_2]^{\beta+}$ complex prefers the three-dimensional structure rather than the two-dimensional one.

Two stationary points have also been located on the $\text{Mg-SHCH}_3]^{\beta+}$ potential energy surface. An eclipsed C_s sym-

TABLE 1: Geometrical Features of the Cys Amino Acid Chain (Protonated and Deprotonated). Geometries of Met Amino Acid Chain Minima Complexes

Geometrical Features of the Cys Amino Acid Chain							
aa chain	X	X-S	S-H	S-C	H-S-H/C ^a	DH(HSCX) ^b	
SH ₂			1.348		92.75		
SHCH ₃	Mg	2.477	1.362		95.36	101.17	
			1.349	1.837	97.05		
SH ⁻	Mg	2.450	1.359	1.872	100.4	103.7	
			1.353				
SCH ₃ ⁻	Al	2.184	1.375		95.4		
	Mg	2.256	1.355		92.8		
				1.851			
	Mg	2.270	—	1.852	116.6		
	Al	2.310	—	1.778	107.8		
Met Amino Acid Chain Minima Complexes Geometries							
aa chain	X	X-S	C1-S	C2-S	C2-C3	DH(C1SC2C3) ^b	DH(C1SC2X) ^b
CH ₃ SCH ₃			1.825	1.825			
CH ₃ SCH ₂ CH ₃	Mg	2.443	1.851	1.851			115.9
			1.826	1.837	1.529	0	
	Al	2.344	1.843	1.890	1.546	138.1	118.9
	Mg	2.406	1.853	1.873	1.535	126.8	114.9

^a Note that the H/C term is C for the methylated and H for the non methylated ligands. ^b DH stands for the dihedral angle.

metry transition state where the imaginary frequency corresponds to the breaking of the Mg-S-C-H plane and an staggered C₁ minimum which is 9 kcal/mol lower in energy (**Mg-1** in Figure 1). The geometrical features of this complex are similar to the nonmethylated structure, Mg-S and S-H bonds lengths are 2.450 and 1.359 Å, respectively, and the Mg lies 103.7° out of the HSC plane, as can be seen in Table 1. The charge transfer is slightly larger than in the nonmethylated complex; here the magnesium has a positive charge of +1.671e⁻ while it was +1.731e⁻ in the nonmethylated structure. This is consistent with the larger electron donor character of the methyl substituent relative to the hydrogen. The charge transfer in these complexes is larger than that observed at the previously studied Mg(II) and Asp, Glu,²³ Asn, and Gln¹⁷ amino acids functional chain complexes. The Bader analysis reports a covalent bond, Mg-S, with an energy density value of -0.003 au slightly larger than the H(*r_c*) of Mg-SH₂²⁺ which agrees with the shorter length of the Mg-S bond. Note that in the previously studied interactions between Asn and Gln amino acid chains and magnesium (II), the bonds formed between the magnesium and the ligand were described as ionic, while the Mg-S bonds here are reported to be covalent. NBO also reports a Mg-S bond formed between the magnesium 3s-orbital contributing with 15.3%, and the out-of-plane sulfur 3p orbital with a contribution of 84.7%. Here again there is a contrast with the earlier-studied Mg-COOY²⁺ complexes representing the *Glu* and *Asp* amino acid functional chains, where the Mg-O bonding was reported to be due to second-order interactions.²³

The binding energies of the magnesium complexes are 79.09 and 96.58 kcal/mol for the nonmethylated and methylated complexes, respectively (energetics are shown in Table 4). These binding energies are significantly lower than the binding energies between the magnesium (II) cation and the previously studied Asp, Glu,²³ Asn and Gln¹⁷ where the binding energies were 375, 376, 130, and 145 kcal/mol, respectively.

Garner and Gresh⁹ performed an ab initio study involving CH₃SH and magnesium (II) interactions, at the HF level of theory, with a 6-631G(2d) basis set for magnesium and SBK-31(2d) for the ligand atoms. They calculated a bond length of 2.42 Å and a binding energy of 90.0 kcal/mol. These values agree reasonably well with our values of 2.450 Å and 96.58 kcal/mol, respectively.

Anionic Form. The Cys chain pK is 8.5, hence in a physiological environment it may lose the terminal hydrogen, thus the deprotonated CH₃S⁻ Cys chain appears as a binding site for some metal cations.¹⁸ In this section we focus on the interactions between this residue and both aluminum (III) and magnesium (II) cations. As we have done in our previous studies, we start with SH⁻ and then add a methyl group to model the Cys deprotonated chain.

The SH⁻ anion has a bond length of 1.354 Å and a negative natural charge of -1.075e⁻ is located on the sulfur atom. After interacting with the cations, angular complexes are formed (see Tables 1 and 2 for the geometry and natural charge distribution values).

The aluminum cation binds to the sulfur, forming a bond of 2.184 Å, and an H-S-Al angle of 95.4°. The sulfur atom loses significant negative natural charge (dropping to -0.094e⁻), which is transferred to the aluminum which has a natural charge of +1.834e⁻. A similar complex is formed between the magnesium (II) and SH⁻ anion. The bond length is 2.256 Å, somewhat larger than the Al-S, while the angle is 92.85°. The charge transfer from the sulfur atom to the magnesium cation is not as large as in the aluminum (III) complex (see Table 2); after complexation with magnesium, the natural charge on sulfur is still -0.649e⁻.

To understand better the binding between the ligand and the cation, Bader topological analysis was performed. The Al-S bond shows a greater charge density at the bond critical point (0.071 au) than the Mg-S bond (0.058 au). Similarly, the energy density at the bond critical point of the Al-S bond (-0.030 au) is 1 order of magnitude more negative than that of Mg-S (-0.003 au) indicating that both are covalent bonds, but with a greater covalent character in the Al-S case. After aluminum binding to the SH⁻, the S-H bond reduces its energy density from -0.184 au to -0.169 au with the corresponding elongation of the bond length. However, for magnesium complexation the S-H bond H(*r_c*) is almost unchanged which is reflected in the bond length of both species (see Table 3 for more details). The NBO analysis reported a double bond between the Al and S atoms, a π bond with contributions of 6 and 94% respectively, and a σ bond with contributions of 50% from both the aluminum 3s orbital and a 3p in-plane sulfur orbital. The magnesium complex, however, is described by a single σ Mg-S bond

TABLE 2: Natural Charges of the Studied Systems

Y	X	X	S	H ^a	C	H _{ip} ^b	H1 ^c	H2 ^d
SH ₂			-0.283	0.141				
	Mg	1.731	-0.240	0.254				
CH ₃ SH			-0.052	0.124	-0.789	0.244	0.237	0.237
	Mg	1.671	-0.062	0.233	-0.735	0.317	0.284	0.293
SH ⁻			-1.075	0.075				
	Al	1.834	-0.094	0.260				
	Mg	1.479	-0.649	0.171				
CH ₃ S ⁻			-0.753		-0.797	0.183	0.183	0.183
	Al	1.585	0.182		-0.821	0.396	0.329	0.329
	Mg	1.395	-0.396		-0.783	0.282	0.251	0.251

methionine aa chain	X	X	S	C1	H _{ip}	H1	H2	C2	H _{ip}	H1	H2	C ₃	H ₃	H2	H1
CH ₃ SCH ₃			0.179	-0.801	0.248	0.232	0.232	-0.8013	0.248	0.232	0.232				
	Mg	1.617	0.167	-0.769	0.289	0.309	0.278	-0.769	0.289	0.309	0.278				
CH ₃ SCH ₃ CH ₃			0.174	-0.799	0.247	0.232	0.232	-0.583		0.232	0.232	-0.668	0.233	0.234	0.234
	Al	1.840	0.540	-0.745	0.351	0.374	0.325	-0.6227		0.348	0.395	-0.967	0.485	0.345	0.331
	Mg	1.649	0.165	-0.754	0.296	0.304	0.271	-0.5977		0.32	0.302	-0.781	0.364	0.244	0.219

^a The hydrogens are bound to the non-hydrogen atom to its left. ^b The subscripts "ip" stands for in-plane (see Figures 1 and 2). ^c "1" indicates the atoms which are behind the paper plane. ^d "2" indicates the atoms pointing out of the paper plane.

formed between the sulfur 3p in-plane orbital (with a contribution of 76.5%) and the magnesium empty 3s orbital.

The methanethiolate is the complete representation of the dehydrogenated Cys chain, which has a S–C bond length of 1.851 Å. The negative charge of the system is distributed between the sulfur and carbon atoms with natural charges of $-0.753e^-$ and $-0.797e^-$, respectively.

Two different rotomers have been located when forming a complex either with aluminum (III) or magnesium (II) cations.

The aluminum binds to the sulfur with an Al–S–C angle of 116.6°, and a bond length of 2.310 Å. The ground state corresponds to the staggered rotomer (see **X-2** in Figure 1), and the second stationary point (2.7 kcal/mol higher in energy) is the eclipsed form, which has an imaginary frequency corresponding to the methyl group rotation. The aluminum has a $+1.585e^-$ charge, while the sulfur and carbon have natural charges of $0.182e^-$ and $-0.821e^-$, respectively (see Table 2). Note that while the charge transfer is larger than in the nonmethylated case, the bond length of the Al–S is also larger.

Similar rotomers have been located for magnesium complexes and the **X-1a** rotomer is also the minimum. The energy difference between the two rotomers is now smaller than in the Al case, only 0.3 kcal/mol. The Mg–S bond length is 2.269 Å with an Mg–S–C angle of 107.8°. The charge distribution is shown in Table 2. Note that the charge transfer from the anion to the cation is larger in the methylated complexes, and much larger in the aluminum than in the magnesium complex. The charge transfer observed in these species is larger than that observed in our previous studies, e.g., the maximum charge transfer observed for the acidic amino acid complexes was in the X–COOCH₂CH₃^{+/2+} complexes with charges of $+2.145$ and $+1.748e^-$ for aluminum and magnesium, respectively.¹⁶ In the acid derivative complexes, the largest charge transfer was also observed in the complexes with the largest chain ligand, corresponding to the **Al-n2.1** and **Mg-bts1** rotomers, with natural charges of $+1.791e^-$ and $+1.833e^-$, respectively.¹⁷

The Bader analysis of the methanethiolate-cation complexes also reports covalent bonds between both aluminum and magnesium sulfur (see Table 3). The aluminum interactions with the SCH₃⁻ results in a more negative energy density for the S–C bond, which is reflected in the shrinking of this bond. Note that the contrary is observed in the magnesium complex, the S–C energy density is slightly less negative, which is

reflected by a small elongation of the S–C bond in Mg–SCH₃⁺. In the Mg–SH₂ complex, when one hydrogen was substituted with CH₃, the H(*r_c*) of the Mg–S became more negative accompanied by S–C shrinking. However, in the dehydrogenated complex, the contrary is observed. After the addition of the methyl group, the energy density of the X–S (for both Mg and Al) is less negative, and the X–S bond is longer in the X–SCH₃^{+/2+} complexes. The NBO description of the Al–S interaction is different for the methylated complex. It reports only a single σ Al–S bond with contributions of 60 and 40% respectively. It also reports a second-order interaction from the sulfur out-of-plane p lone-pair to the aluminum out-of-plane empty p orbital, which has an energetic contribution of 14.42 kcal/mol. In the magnesium complex, the Mg–S bond is described in a similar manner with a slightly larger contribution from the magnesium 3s orbital, 27%. It is interesting to note that the Bader analysis, reporting a higher electron density for the Al–S bond of Al–SH²⁺ than that of Al–SCH₃²⁺, the NBO, which indicated a double bond in the nonmethylated case, and the simple bond length of the Al–S bond are all in agreement that the Al–S bond itself is stronger in the nonmethylated case than that in the methylated case. Similar arguments apply to the Mg complexes, though the differences are minimal.

In comparing to the aluminum complexes, we have observed numerous evidences of weaker Mg–ligand interactions, larger X–S bond lengths, smaller charge transfer, and smaller H(*r_c*) values. This is also clearly reflected in the binding energies of these complexes. Al–SH²⁺ has a binding energy of 702.35 kcal/mol while the magnesium complex binding energy is only 351.56 kcal/mol. Similarly, the tiomethylate complexes have binding energies of 741.38 and 359.59 kcal/mol for Al(III) and Mg(II), respectively (see Table 4). Note that after the methyl group is added, the binding energy increase is much larger for the aluminum complex. These binding energies are comparable to the binding energies of these cations with Asp and Glu,¹⁶ and larger than the binding energies with Asn and Gln.¹⁷

The increase in binding energy upon methyl substitution at first glance appears contrary to the data mentioned above comparing the Al–S bonds in the two complexes. NBO, the Bader analysis, and bond length all agree that the Al–S bond is weaker in Al–SCH₃²⁺ than in that Al–SH²⁺. However, the binding energy of the methylated species is about 40 kcal/

TABLE 3: Bader Analysis for the Studied Complexes^a

		X-S	S-H	S-C					
SH ₂	ρ		0.212						
	$\nabla^2\rho$		-0.566						
	$G(r)$		0.056						
	$H(r)$		-0.197						
X-SH ₂	Mg	ρ	0.037	0.214					
		$\nabla^2\rho$	0.124	-0.609					
		$G(r)$	0.033	0.035					
		$H(r)$	-0.002	-0.187					
SHCH ₃		ρ		0.212	0.172				
		$\nabla^2\rho$		-0.565	-0.272				
		$G(r)$		0.058	0.045				
		$H(r)$		-0.199	-0.113				
X-SHCH ₃	Mg	ρ	0.039	0.216	0.155				
		$\nabla^2\rho$	0.131	-0.607	-0.189				
		$G(r)$	0.035	0.0384	0.045				
		$H(r)$	-0.003	-0.190	-0.092				
SH ⁻		ρ		0.196					
		$\nabla^2\rho$		-0.451					
		$G(r)$		0.071					
		$H(r)$		-0.184					
X-SH ⁻	Al	ρ	0.071	0.208					
		$\nabla^2\rho$	0.104	-0.582					
		$G(r)$	0.056	0.032					
		$H(r)$	-0.030	-0.178					
X-SH ⁻	Mg	ρ	0.051	0.208					
		$\nabla^2\rho$	0.217	-0.536					
		$G(r)$	0.058	0.052					
		$H(r)$	-0.003	-0.186					
SCH ₃ ⁻		ρ			0.162				
		$\nabla^2\rho$			-0.234				
		$G(r)$			0.051				
		$H(r)$			-0.109				
X-SCH ₃ ⁻	Al	ρ	0.058		0.187				
		$\nabla^2\rho$	0.034		-0.290				
			0.033		0.058				
		$H(r)$	-0.024		-0.131				
X-SCH ₃ ⁻	Mg	ρ	0.050		0.164				
		$\nabla^2\rho$	0.205		-0.228				
		$G(r)$	0.054		0.0439				
		$H(r)$	-0.003		-0.101				
		C1-S	C2-S	C2-C3	S-X	X-C3			
CH ₃ SCH ₃		ρ	0.177	0.177					
		$L^2\rho$	-0.291	-0.291					
		$G(r)$	0.047	0.047					
		$H(r)$	-0.120	-0.120					
CH ₃ SCH ₂ CH ₃		ρ	0.177	0.175	0.244				
		$L^2\rho$	-0.289	-0.276	-0.558				
		$G(r)$	0.047	0.046	0.056				
		$H(r)$	-0.119	-0.115	-0.195				
X-CH ₃ SCH ₂ CH ₃	Al	ρ	0.160	0.157	0.233	0.060	0.047		
		$L^2\rho$	-0.187	-0.193	-0.502	0.035	0.114		
		$G(r)$	0.055	0.044	0.057	0.035	0.041		
		$H(r)$	-0.101	-0.092	-0.181	-0.026	-0.012		
X-CH ₃ SCH ₂ CH ₃	Mg	ρ	0.163	0.163	0.241	0.041			
		$L^2\rho$	-0.219	-0.221	-0.541	0.156			
		$G(r)$	0.046	0.043	0.055	0.041			
		$H(r)$	-0.100	-0.098	-0.190	-0.002			

^a Charge densities (ρ), laplacian of the densities ($\nabla^2\rho$), and energy densities ($H(r)$) of the corresponding X bond critical points.

mol greater than that of Al-SH²⁺. This emphasizes the importance of charge delocalization over the entire complex, rather than just considering the Al-S bond itself. The difference in natural charge distribution between the two complexes is significant, demonstrating the capacity of the larger ligand to transfer more charge to the Al(III) cation. This explains the apparent conflict between bond strength indicators and calculated binding energy. It also indicates why the effect of the methyl group is smaller in the case of binding the less positively charged Mg(II) cation.

TABLE 4: Energies of the Minima Structures E (in hartrees)^a

amino acid chain	X	E	BE
SH ₂		-399.378591	
	Mg	-598.732064	-79.09
CH ₃ SH		-438.662434	
	Mg	-638.043775	-96.58
SH ⁻		-398.825102	
	Al	-640.331752	-702.35
SCH ₃ ⁻		-598.612619	-351.46
	Mg	-438.098252	
CH ₃ SCH ₃		-679.667089	-741.38
	Al	-637.899861	-360.3
CH ₃ SCH ₂ CH ₃		-477.946065	
	Mg	-677.34703	-109.37
CH ₃ SCH ₂ CH ₃		-517.234846	
	Al	-758.231032	-382.74
	Mg	-716.653255	-120.31

^a BE is the binding energy of the aminoacid chains with the corresponding metal cation (in kcal/mol).

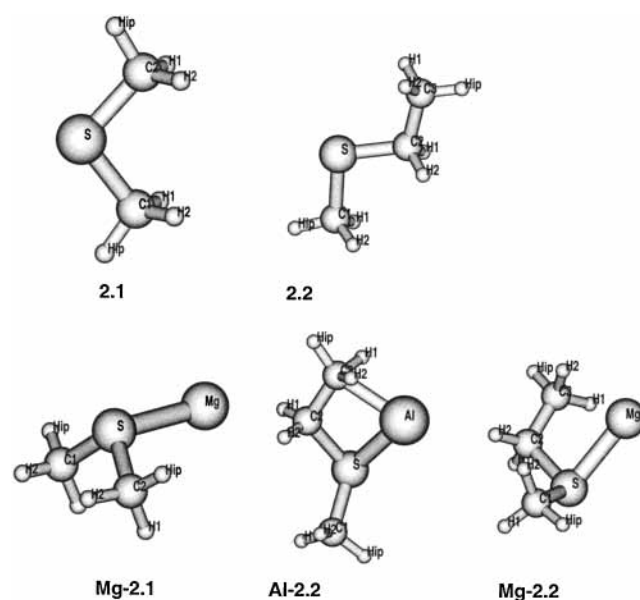


Figure 2. 2.1 is the simplest functional group of the Met amino acid chain and the 2.2 is the complete chain of the Met amino acid. The complexes below are the corresponding ground states after metal binding to the Met chain.

Garmer and Gresh⁹ have also reported data concerning the deprotonated *Cys* chain and magnesium interactions. They calculated a bond length of 2.24 Å and a binding energy of 349 kcal/mol which agree well with our predictions.

X-Methionine Amino Acid Chain Interactions. Methionine is the second sulfur containing amino acid, and its functional chain is CH₃SCH₂CH₃. According to our strategy, we have first studied the CH₃SCH₃ group, and then the complete chain interactions with the metal cations.

Two stationary points were located for the CH₃SCH₃ chain. The minimum is shown in Figure 2, (2.1) while the rotomer has an imaginary frequency and lies 1.69 kcal/mol higher in energy than 2.1. The ground-state structure has a C_s symmetry with C-S bond length of 1.825 Å and a C-S-C angle of 99.6°.

No Al-CH₃SCH₃ complexes have been located. However, magnesium was found to complex with this residue.

Two stationary points were located on the Mg-CH₃SCH₃²⁺ potential energy surface; a C_{2v} symmetry transition state, where the magnesium binds to the sulfur atom in the C-S-C plane, and the C_s symmetry ground state, **Mg-2.1** which lies 8.26

kcal/mol lower in energy and has a Mg–S bond length of 2.443 Å. After the addition of the magnesium cation, the S–C bonds elongate slightly from 1.825 Å to 1.851 Å, while the C–S–C angle is 4° larger (see Table 1). The natural charge distribution also changes slightly after the interaction between the CH₃SCH₃ chain with the magnesium cation. There is a charge transfer from the ligand to the magnesium cation, and all the atoms of the ligand have a more positive natural charge than in the CH₃SCH₃ (see Table 2 for more details). The Mg–S bond is covalent according to the Bader analysis, since the energy density value at the bond critical point is negative (−0.003 au). The NBO Analysis also reports a bond between the magnesium 3s and a sulfur p orbital, with contributions of 17.5% and 82.5%, respectively.

While magnesium (II) has been seen to form complexes with these ligands, aluminum (III) does not form stable complexes with SH₂, HSCH₃ or CH₃SCH₃. We have investigated further these complexes, and observed that this happens because of the strong aluminum sulfur interactions. We have two different interaction modes corresponding to the **Mg-2.1**; C_s and to the C_{2v} transition state rotomer. Let us examine the molecular orbitals of these two structures when interacting with the magnesium (II) and aluminum (III) cations placed at arbitrary distances first along the C_s symmetry plane and then along the axis of C_{2v} symmetry. Starting from the former structure, we have observed a charge transfer followed by the aluminum cation moving away. On the other hand, the second possibility leads to a fragmentation of the complex into Al–S⁺ and two CH₃⁺ moieties. If we examine the Molecular Orbitals of these structure, a strong π interaction is observed between the aluminum and the sulfur (see Figure 3a) hence, an Al–S⁺ complex is formed leading to S–C bond breaking. In the **Mg-2.1** structure, however, this interaction is almost nonexistent (see Figure 3b), thus an MgCH₃SCH₃²⁺ complex is found. Similar arguments apply to the X-SHCH₃ and X-SH₂ cases and the same has been observed for the following levels of theory: MP2(full) with 6-31++G** and aug-cc-PVTZ basis sets, B3PW91 with 6-31++G** and 6-31++G(2df,2p) basis sets and finally for CCSD with 6-31++G**, cc-PVTZ and 6-311++G(2df,2p) basis sets.

After adding a methyl group to simulate more accurately the methionine chain, three rotomers were located in an energy range of 3 kcal/mol, a minimum (**2.2**) and two transition state rotomers. The geometry of the minimum is shown in Table 1. The S–C bonds are slightly larger than those in CH₃SCH₃, and the new C–C bond length is 1.529 Å.

An Al–CH₃SCH₂CH₃ complex was located (**Al-2.2** in Figure 2). The interaction with the aluminum forms a four-membered ring between the Al, S, C2 and C3. The bond lengths of Al–S and Al–C are 2.345 and 2.170 Å respectively. The C1–S and S–C2 bond lengths elongate upon complexation (see Table 1), while the C2–C3 bond length is nearly unchanged. The formation of this ring alters substantially the natural charge distribution of the CH₃SCH₂CH₃ chain. Negative charge is transferred to the aluminum, resulting in a final natural charge of +1.840e[−]. The C2 and C3 atoms show higher negative charges in the complex than in the ligand, while the sulfur gains in positive charge changing from +0.174 e[−] in the CH₃SCH₂CH₃ chain, to +0.540 e[−] after complexation with the aluminum. Similarly, the rest of the atoms also have a more positive natural charge (see Table 2). The Bader analysis of this complex reports covalent bonds for both the Al–S and Al–C3 interactions with energy density values of −0.026 and −0.012 au respectively (see Table 2). The formation of the ring reduces

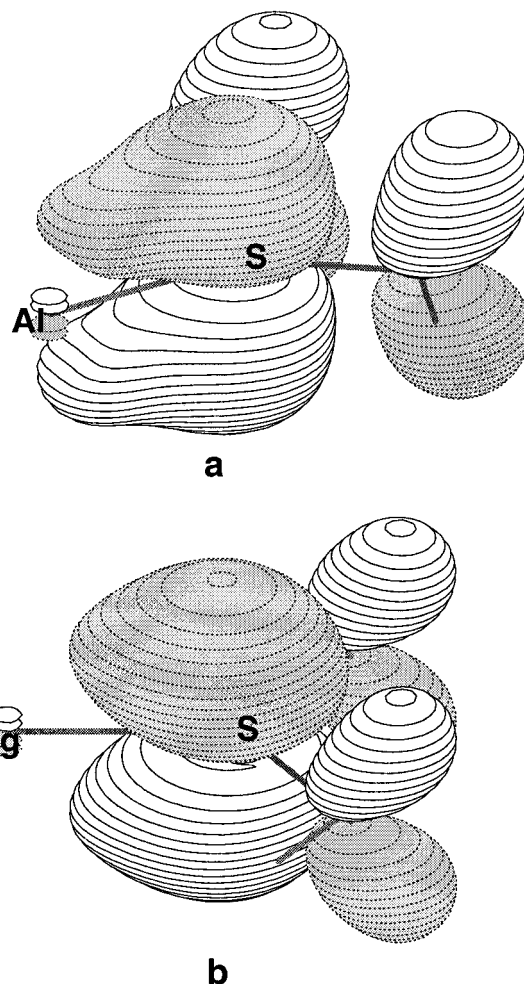


Figure 3. π interactions between the metal cation and the CH₃SCH₃ ligand. (a) for the aluminum (III) cation and (b) for magnesium (II).

the energy density of the C1–S, S–C2 and C2–C3 bonds reflected by an elongation of these bonds. The NBO description of this complex is reported with an Al–S bond, with contributions of the 42.2 and 58.8% respectively, while the Al–C is reported as a second-order interaction coming from the terminal CH₃ moiety C–H bonds to the aluminum empty p-orbitals. The sum of these energetic contributions had an overall value of 30 kcal/mol.

Two CH₃SCH₂CH₃–Mg complexes were found; a C_s symmetry transition state with a negative frequency corresponding to the magnesium vibration out of the C–S–C plane, and the 8.24 kcal/mol lower in energy C₁ symmetry ground state. This structure is depicted in Figure 2 (**Mg-2.2**). The complex is similar to the **Al-2.2** but the Mg and C3 atoms are too far apart to interact with each other. The Mg–S bond length is 2.406 Å, slightly larger than the Al–S bond. The charge redistribution of this complex is not as important as it was in the aluminum complex, indicating the weaker complexation with magnesium. Mg has a final natural charge of +1.647e[−] while the S atom only changes by −0.010e[−] (see Table 2). The Bader analysis also reports a covalent bond between the magnesium and the sulfur, with a value for H(*r*_c) of −0.0021 au. The effect of the magnesium on the adjacent C1–S and S–C2 bonds is to increase their energy density (see Table 3). Thus, their bonds elongate, while the H(*r*_c) for the C2–C3 is more negative, and that bond shrinks. NBO analysis also reports a bond and it is described as a σ bond occurring between the Mg 3s -orbital

with a contribution of 14% and the sulfur's out-of-CSC-plane *p* orbital.

The binding energy for the $\text{Mg}-\text{CH}_3\text{SCH}_3]^{2+}$ is 109.37 kcal/mol and the $\text{X}-\text{CH}_3\text{SCH}_3\text{CH}_2]^{+3/2}$ binding energies are 382.74 and 120.31 kcal/mol for aluminum (III) and magnesium (II), respectively. These binding energies are larger than those of the Cys chain complexes, and comparable to the binding energies of the Asn and Gln amino acid chain with aluminum (III) and magnesium (II) cations.

Note that for the cases which give enough information for comparison, the substitution of one H of SH_2 for a methyl group increases the binding energy of the Mg complex by 17.49 kcal/mol. The substitution of the second H by CH_3 raises complexation energy by 12.81 kcal/mol and substitution of one of the methyls of $\text{S}(\text{CH}_3)_2$ by an ethyl group results in a Mg binding energy 10.94 kcal/mol higher. Comparing the two anionic ligands, the substitution of the hydrogen of SH^- for a methyl group increased the Mg binding energy by only 8.84 kcal/mol and the Al binding energy by 39.03 kcal/mol.

Conclusions

We have studied the interactions between the sulfur containing amino acid chains with magnesium (II) and aluminum (III) cations. The three different models studied, reflect significant differences comparing with the previously studied acid and acid derivative amino acid chain complexes.

The weakest binding among these complexes occurs in the Cys amino acid chain (note that no aluminum (III) complexes were found). The $\text{Mg}-\text{SH}_2]^{2+}$ and $\text{Mg}-\text{CH}_3\text{SH}]^{2+}$ binding energies are 79.09 and 96.58 kcal/mol, respectively, and are the weakest interactions we have found for the systems studied so far.^{16,17} The dehydrogenated Cys chain interactions are comparable to the binding energies calculated for the acidic group amino acid chains¹⁶ (Glu and Asp). The binding energies for aluminum (III) and magnesium (II) with the $\text{CH}_3\text{S}]^-$ are 741 and 360 kcal/mol, respectively. Finally, the binding energies calculated for the Met chain, are significantly lower than the acidic group amino acid chains. At 382 and 120 kcal/mol for binding Al and Mg, respectively, they are similar to the binding energies of the acid derivative amino acid chains¹⁷ (Gln and Asn).

The charge transfer observed in these complexes is also the largest observed through this series of studies. The positive charge on the metal in these complexes is the smallest observed after binding to the ligand.

Throughout this series of studies, lengthening the ligand chain has led to more stably bound complexes. There has also been a trend of diminishing returns as the chain grows longer, as is well demonstrated by the Mg complexes of this work. Larger chains allow for greater charge redistribution and in some cases ring formation (such as in the $\text{Al}-\text{CH}_3\text{SCH}_2\text{CH}_3]^{2+}$ case seen here). It should be remembered that even though a specific bond appears to be weaker than another, the binding energy of these complexes is not determined by the metal-sulfur bond alone. The Al-S bond in $\text{Al}-\text{SH}]^{2+}$ is by all indications weaker than that same bond in $\text{Al}-\text{SCH}_3]^{2+}$, but the binding energy of the second complex is 39 kcal/mol larger than that of the first. This demonstrates the importance of charge delocalization through the entire complex.

It is also important to point out that the magnesium (II) cation interactions with the sulfur containing ligands studied in the present work, are described to be covalent by the Bader analysis, while the interactions with the acid derivative amino acids were reported to be ionic.¹⁷ Similarly, the NBO analysis reports a

bond for all the Mg-S interactions. However, the magnesium (II) interactions with the acidic amino acid chains CH_3COO^- and $\text{CH}_3\text{C}_2\text{COO}^-$ were reported to be second-order interactions between the metal and the ligand.¹⁶

Acknowledgment. J.M.M. and J.E.F. thank the Basque Government (Eusko Jaurlaritz) for a grant. Financial support from the Spanish DGICYT Grant No. PB96/1524 and from the Provincial Government of Gipuzkoa (Gipuzkoako Foru Aldundia) is gratefully acknowledged.

References and Notes

- (1) Williams, R. J. P. *Coord. Chem. Rev.* **1996**, *149*, 1.
- (2) Pohlmeier, A.; Knoche, W. *Int. J. Chem. Kinet.* **1996**, *28*, 125–136.
- (3) Candy, J. M.; McArthur, F. K.; Oakley, A. E.; Taylor, G. A.; Mountfort, C. P. L.; Thompson, J. E.; Beyreuther, P. R. C. H. E. B. K.; Perry, G.; Ward, M. K.; Martyn, C. N.; Edwardson, J. A. *J. Neurol. Sci.* **1992**, *107*, 210–218.
- (4) Meri, H.; Banin, E.; Roll, M.; Rousseau, A. *Prog. Neurobiol.* **1993**, *40*, 89–121.
- (5) Bhattacharyya, M. H.; Wilson, A. K.; Silbergeld, E. K.; Watson, L.; Jeffrey, E. *Metal Induced Osteotoxicities* **1995**, *525*, 363–441.
- (6) Macdonald, T. L.; Martin, R. B. *Trends Biochem. Sci.* **1988**, *13*, 15–19.
- (7) Martin, R. B. *Clin. Chem.* **1986**, *32*, 1797.
- (8) Ganrot, P. O. *Environ. Health. Perspect.* **1986**, *65*, 363.
- (9) Garmer, D. R.; Gresh, N. *J. Am. Chem. Soc.* **1994**, *116*, 3556–3567.
- (10) Gresh, N.; Stevens, W. J.; Krauss, M. *J. Comput. Chem.* **1995**, *16*, 843–855.
- (11) Gresh, N.; Garmer, D. R. *J. Comput. Chem.* **1996**, *17*, 1481–1495.
- (12) Deerfield, D. W.; Fox, D. J.; Headgordon, M.; Hiskey, R. G.; Pedersen, L. G. *Proteins: Struct., Funct., Genet.* **1995**, *21*, 244–255.
- (13) Tortajada, J.; Leon, E.; Morizur, J.-P.; Luna, A.; Mo, O.; Yanez, M. *J. Phys. Chem.* **1995**, *99*, 13890–13898.
- (14) Tortajada, J.; Leon, E.; Luna, A.; Mo, O.; Yanez, M. *J. Phys. Chem.* **1994**, *98*, 12919–12926.
- (15) Luna, A.; Amekraz, B.; Tortajada, J.; Morizur, J. P.; Alcamí, M.; Mo, O.; Yanez, M. *J. Am. Chem. Soc.* **1998**, *120*, 5411–5426.
- (16) Mercero, J. M.; Fowler, J. E.; Ugalde, J. M. *J. Phys. Chem. A* **1998**, *102*(35), 7006–7012.
- (17) Mercero, J. M.; Fowler, J. E.; Ugalde, J. M. *J. Phys. Chem. A* **2000**, *104*, 7053–7060.
- (18) Fersht, A. R. *Enzyme Structure and Mechanism*; Freeman: New York, 1985.
- (19) Roques, B. P.; Fournie-Zaluski, M. C.; Saroca, E.; Lecomte, J. M.; Malfroy, B.; Llorens, C.; Schwartz, J. C. *Nature* **1980**, *288*, 286.
- (20) Roques, B. P.; Noble, F.; Gauge, V.; Fournie-Zaluski, M. C.; Beaumont, A. *Pharmacol. Rev.* **1993**, *45*, 88.
- (21) Frisch, M. J.; Trucks, G. W.; Schlegel, H. B.; Gill, P. M. W.; Johnson, B. G.; Robb, M. A.; Cheeseman, J. R.; Keith, T.; Petersson, G. A.; Montgomery, J. A.; Raghavachari, K.; Al-Laham, M. A.; Zakrzewski, V. G.; Ortiz, J. V.; Foresman, J. B.; Peng, C. Y.; Ayala, P. Y.; Chen, W.; Wong, M. W.; Andres, J. L.; Replogle, E. S.; Gomperts, R.; Martin, R. L.; Fox, D. J.; Binkley, J. S.; Defrees, D. J.; Baker, J.; Stewart, J. P.; Head-Gordon, M.; Gonzalez, C.; Pople, J. A. *Gaussian 94*, version b.2; Gaussian, Inc.: Pittsburgh, PA, 1994.
- (22) Frisch, M. J.; Trucks, G. W.; Schlegel, H. B.; Scuseria, G. E.; Robb, M. A.; Cheeseman, J. R.; Zakrzewski, V. G.; Montgomery, J. A.; Stratmann, R. E.; Burant, J. C.; Dapprich, S.; Millam, J. M.; Daniels, A. D.; Kudin, K. N.; Strain, M. C.; Farkas, O.; Tomasi, J.; Barone, V.; Cossi, M.; Cammi, R.; Mennucci, B.; Pomelli, C.; Adamo, C.; Clifford, S.; Ochterski, J.; Petersson, G. A.; Ayala, P. Y.; Cui, Q.; Morokuma, K.; Malick, D. K.; Rabuck, A. D.; Raghavachari, K.; Foresman, J. B.; Cioslowski, J.; Ortiz, J. V.; Stefanov, B. B.; Liu, G.; Liashenko, A.; Piskorz, P.; Komaromi, I.; Gomperts, R.; Martin, R. L.; Fox, D. J.; Keith, T.; Al-Laham, M. A.; Peng, C. Y.; Nanayakkara, A.; Gonzalez, C.; Challacombe, M.; Gill, P. M. W.; Johnson, B. G.; Chen, W.; Wong, M. W.; Andres, J. L.; Head-Gordon, M.; Replogle, E. S.; Pople, J. A. *Gaussian 98*, version a.5; Gaussian, Inc.: Pittsburgh, PA, 1998.
- (23) Labanowsky, J.; Andelzelm, J. *Density Functional Methods in Chemistry*; Springer-Verlag: New York, 1991.
- (24) Tschinke, V.; Ziegler, T. *Theor. Chim. Acta* **1991**, *81*, 651.
- (25) Johnson, B. G.; Gill, P. M. W.; Pople, J. A. *J. Chem. Phys.* **1993**, *98*, 5612.
- (26) Becke, A. D. *J. Chem. Phys.* **1993**, *98*, 5648.
- (27) Lee, C.; Yang, W.; Parr, R. G. *Phys. Rev. B* **1988**, *37*, 785.

(28) Reed, A. E.; Curtiss, L. A.; Weinhold, F. *Chem. Rev.* **1988**, 88, 899.

(29) Bader, R. F. W. *Atoms in Molecules: A Quantum Theory*; Clarendon Press, Science Publications: Oxford, 1990; Chapter 7.

(30) Foster, J. P.; Curtiss, L. A.; Weinhold, F. *J. Am. Chem. Soc.* **1980**, 88, 899.

(31) For the Nbo version 3.1, see: Glendening, E. D.; Reed, A. E.; Carpenter, J. E.; Weinhold, F.

(32) Biegler-Koning, F. W.; Bader, R. F. W.; Tang, T. H. *J. Comput. Chem.* **1980**, 27, 1924.

(33) Molden. See <http://www.cmbi.kun.nl/schaft/molden/molden.html>.